Localization-landscape generalized Mott-Berezinskiĭ formula

Gabriel Hayoun [1,*] Ilya A. Gruzberg [2,†] and Marcel Filoche [1,‡]
[1]*Institut Langevin, ESPCI Paris, PSL University, CNRS, Paris, France*
[2]*Department of Physics, The Ohio State University, Columbus, Ohio 43210, USA*

(Received 30 December 2025; accepted 18 February 2026; published 16 March 2026)

We introduce a conceptual reformulation of the Mott-Berezinskiĭ (MB) theory of low-frequency ac conductivity in disordered systems based on localization-landscape theory. Instead of assuming uniform localization and fixed hopping distances, transport is described through an effective potential whose geometry encodes the spatial organization and energy-dependent localization of quantum states. Using the associated Agmon metric, we define a generalized Mott scale that replaces the classical hopping length with a geometric criterion set by the disorder landscape. This framework naturally incorporates strong spatial inhomogeneity and yields the ac conductivity directly from the effective potential. The standard MB result is recovered as a limiting case. Our approach extends the conceptual foundation of MB theory to arbitrary disordered media and energies approaching the mobility edge, providing a unified description of ac transport in complex quantum materials.

DOI: 10.1103/tglp-ts2c

I. INTRODUCTION

In lightly doped semiconductors displaying some form of quenched disorder, whether this disorder originates from a random spatial alloy composition or from the distribution of impurities, the electronic states near the Fermi energy that contribute to the conduction at low temperature can be either extended or localized, the two regimes being separated by the so-called *mobility edge*. On the localized side, electronic transport occurs via electron hopping between localized states, and can be modeled by a network of random resistors and capacitors [1] and investigated through percolation theory [2–5]. The low-temperature conductivity of Weyl semimetals and weakly doped semiconductors can also be derived from a renormalization scheme developed to study localization-delocalization phase transition [6].

At low temperatures, the phonon-assisted hopping progressively leads to vanishing dc conductivity at $T = 0$, while the ac transport relies on photon-assisted hopping [7–9]. In d dimensions, in the low-frequency limit, the ac conductivity $\sigma(\omega)$ is described by the Mott-Berezinskiĭ (MB) formula, first proposed by Mott (with contributions by Halperin and Anderson) based on intuitive physical arguments [10–13]:

$$\sigma(\omega) \underset{\omega \longrightarrow 0}{\sim} 2\pi e^2 \hbar\, \nu^2 \xi^{d+2} \omega^2 \left(\ln \frac{2\Delta_\xi}{\hbar\omega} \right)^{d+1}, \qquad (1)$$

where ν is the density of states at the Fermi energy E_F, ξ is the localization length of these states, and $\Delta_\xi = (\nu \xi^d)^{-1}$ is the mean level spacing within the localization volume. In this limit, the main dependence on the frequency ω is quadratic, with a logarithmic correction whose power depends on d. The MB formula was rigorously derived by Berezinskiĭ in one dimension (1D) [14].

The MB formula relies on several assumptions that are critical for its proper derivation:

(1) The Fermi energy lies in the part of the spectrum where electronic states are Anderson localized [15].

(2) The states contributing to $\sigma(\omega)$ are located in spatially distinct wells of the random potential.

(3) The localization length ξ of the relevant states is uniform across the system.

(4) Finally, although the MB formula is expressed in any dimension, Berezinskiĭ's mathematical derivation was only one-dimensional.

This formula was rederived in 1D using various methods: the phase formalism [16,17], instantons and supersymmetry [18,19], and correlations of electronic wave functions [20,21]. Recent work focused on an expansion in the density of potential wells and asymptotic formulas of the correlators [22] to recover the MB formula. A rigorous upper bound on $\sigma(\omega)$ (consistent with the MB expression) was obtained in Ref. [23]. Corrections to Eq. (1) and its extension to a broader range of ω was achieved for a Gaussian white noise [24] using the instanton approach and a modern method to compute correlation functions with functional determinants [25]. The latter method was generalized to quasi-1D wires [26].

The goal of the present work is to generalize the MB formula to any type of disorder, relaxing the requirement of a uniform localization length and the presence of well-defined wells in the disordered potential. We achieve these goals using the localization-landscape (LL) theory.

II. THE LOCALIZATION LANDSCAPE APPROACH

The LL theory, introduced in 2012 by the third author and Mayboroda [27], provides a mathematical framework to study the properties of quantum states in disordered and complex

*Contact author: gabriel.hayoun@espci.psl.eu
†Contact author: gruzberg.1@osu.edu
‡Contact author: marcel.filoche@espci.psl.eu

systems without having to solve the Schrödinger equation. If $\hat{H}$ is the Hamiltonian of the system, the LL function u is defined as the solution to the associated Dirichlet problem:

$$\hat{H}u = 1. \tag{2}$$

A cornerstone achievement of the LL theory is the discovery that the reciprocal of the LL function, $V_u \equiv 1/u$, acts as a true *effective potential*. This emergent potential provides direct, quantitative access to the physics of localization: it delineates localization regions, predicts the integrated density of states of $\hat{H}$ [28], and determines the localization lengths of its eigenstates [29,30]. The LL framework has demonstrated practical impact by enabling large-scale, predictive simulations of carrier transport in highly disordered semiconductors, in particular nitride-based alloys, while achieving ∼100-fold reduction in computational cost compared to conventional quantum-mechanical approaches [31–33]. Recently, the LL was used to provide a physically grounded model of variable-range-hopping transport in disordered semiconductors, overcoming the simplifications of the Miller-Abrahams model [34].

In the following, we consider a spatial region Ω in d dimensions in which electrons move in a time-independent (quenched) disorder potential $V(\boldsymbol{r})$. We allow for the effective mass of electrons to be a position-dependent quantity $m_e^*(\boldsymbol{r})$. Then, electronic wave functions ψ satisfy the time-independent Schrödinger equation:

$$\hat{H}\psi = -\frac{\hbar^2}{2}\mathrm{div}\left(\frac{1}{m_e^*}\boldsymbol{\nabla}\psi\right) + V\psi = E\psi. \tag{3}$$

We do not assume that the potential V itself exhibits clearly defined and spatially separated wells. Rather, we require this property to hold for the effective potential V_u derived from Eq. (2). This is a significantly weaker assumption, as V_u is much smoother than V, a consequence of u being a solution to a second-order partial differential equation. The regions surrounding the minima of V_u are referred to hereafter as basins and denoted by B_i. These basins are defined as the areas around each minimum bounded by the level set $V_u = E$. Their extent therefore depends on the energy E under consideration.

We also assume that the basins of V_u at energy E_F are well separated and nonpercolating. Since, in the lower part of the spectrum of $\hat{H}$, electronic states are Anderson localized within these basins [35], this amounts to assuming that as in Mott's original hypothesis, the Fermi level lies in this localized regime. However, unlike in the MB derivation, we do not require all states to share an identical localization length ξ. Finally, V_u is assumed to be statistically isotropic and homogeneous.

Our goal is to compute asymptotically the ac conductivity $\sigma(\omega)$ in the limit $\omega \to 0$ when the density of states per unit volume, $\nu(E)$, can be taken as a constant ν in the range $[E_F - \hbar\omega, E_F + \hbar\omega]$. The statistical isotropy of the medium ensures that the average conductivity is the same in all directions of space. The ac conductivity is given by the Kubo-Greenwood (KG) formula:

$$\sigma(\omega) \underset{\omega\longrightarrow 0}{\approx} \frac{2\pi e^2\hbar}{d}|\Omega|\nu^2\omega^2\,|\boldsymbol{X}|^2_{\mathrm{avg}}, \tag{4}$$

where $|\Omega|$ is the volume of the system and $|\boldsymbol{X}|^2_{\mathrm{avg}}$ is the squared position matrix element, averaged over all possible initial and final states [17]. The matrix element of x_α (the position along axis α) between any initial and final states (i, j) reads

$$X^{(\alpha)}_{j,i} = \langle\psi_j|\hat{x}_\alpha|\psi_i\rangle = \int \psi_j^*(\boldsymbol{r})\, x_\alpha\, \psi_i(\boldsymbol{r})\,\mathrm{d}\boldsymbol{r}, \tag{5}$$

with $|\boldsymbol{X}_{j,i}|^2 = \sum_{\alpha=1}^{d} |X^{(\alpha)}_{j,i}|^2$.

III. THE LL-GENERALIZED MOTT SCALE

The first step of the derivation is to determine which pairs of states (i, j) contribute to the conduction at frequency ω. To this end, we generalize the criterion introduced by Mott and Berezinskiĭ based on the spatial separation between states localized in two basins, B_i and B_j. We define the two-well Hamiltonian $\hat{H}^{(2)}_{i,j}$ as the projection of $\hat{H}$ onto the subspace spanned by $\psi^{(1)}_i$ and $\psi^{(1)}_j$, the localized eigenstates of the one-well Hamiltonians associated with each basin. The Hamiltonian $\hat{H}^{(2)}_{i,j}$ is thus a 2×2 matrix whose off-diagonal element t_{ij} is given by the overlap integral:

$$t_{ij} = t^*_{ji} \approx E_F \int_\Omega \psi^{(1)*}_j(\boldsymbol{r})\, \psi^{(1)}_i(\boldsymbol{r})\,\mathrm{d}\boldsymbol{r}. \tag{6}$$

The two states hybridize and form bonding and antibonding states ψ_+ and ψ_- [21], with the energy splitting

$$\Delta E = E_+ - E_- = \sqrt{4t_{ij}^2 + (E_i - E_j)^2}. \tag{7}$$

A pair of states (i, j) contributes to $\sigma(\omega)$ only if the energy splitting satisfies the resonance condition:

$$\Delta E = \hbar\omega. \tag{8}$$

When the overlap integrals are small, hybridization has minimal impact on the wave functions. As a result, the single-well wave function $\psi^{(1)}_i$ is nearly identical to the system's wave function localized within the basin B_i. Nevertheless, even for small t_{ij}, the basins B_i and B_j cannot contribute to the ac conductivity if they are too close to each other, since then ΔE fails to satisfy the resonance condition. Therefore, we must obtain precise estimates of the overlap t_{ij}, which we are going to do using the LL.

A salient point of our approach is that V_u, contrary to the original potential, provides in general very good estimates for the rate of decay of wave functions [29]. These estimates use the so-called Agmon distance ρ_E [36,37], defined as

$$\rho_E(\boldsymbol{r}_1, \mathbf{r}_2) = \min_{\gamma(\boldsymbol{r}_1,\boldsymbol{r}_2)} \int_\gamma \sqrt{\frac{2m}{\hbar^2}[\,V_u(\boldsymbol{r}) - E\,]_+}\,\mathrm{d}s, \tag{9}$$

where $[x]_+ = \max(x, 0)$. The minimum is computed over all possible paths between points $\boldsymbol{r_1}$ and $\boldsymbol{r_2}$, E being the energy of the state considered. The path that minimizes the Agmon distance is a *geodesic* of the implicit metric inside the integral. For a constant potential, this geodesic is simply a straight line between the two points, and the Agmon distance reduces to the usual term $\sqrt{2m(V-E)/\hbar^2}\,|\boldsymbol{r_2} - \boldsymbol{r_1}|$ that appears in quantum tunneling.

With the Agmon distance at hand, we can characterize the exponential decay of any localized wave function outside its basin, provided there are no resonances in distant basins [29]:

$$\psi_i(\boldsymbol{r}) \approx c_i \exp(-\rho_{E_i}(\boldsymbol{r}, B_i)) \quad \text{outside } B_i. \tag{10}$$

The detailed structure of ψ_i inside the basin is not important for what follows, but we can assume that $|\psi_i(\boldsymbol{r})| \sim c_i$ inside B_i. Due to the exponential decay outside B_i, the normalization constant c_i is roughly $V_i^{-1/2}$, where V_i is the localization volume occupied by the state ψ_i.

Let us consider two localized states indexed by i and j: to ensure energy conservation for photon-assisted hopping, we require $\Delta E = \hbar\omega$, see Eq. (8). Their energies are thus bounded by $E_F - \hbar\omega \leqslant E_{i,j} \leqslant E_F + \hbar\omega$ and, as $\hbar\omega$ tends to zero, we have $E_i \approx E_j \approx E_F$. Agmon distances associated with both energies therefore become almost identical to the Agmon distance associated with E_F. From now on, we will only consider this Agmon distance, hereafter denoted ρ (removing the subscript E_F).

Plugging Eq. (10) into Eq. (6) for t_{ij} leads to the computation of an integral of $\exp(-\rho(\boldsymbol{r}, B_i) - \rho(\boldsymbol{r}, B_j))$ mostly supported around the geodesic of the Agmon distance connecting basins B_i and B_j. This results in the estimate (see Appendix A for details)

$$t_{ij} \propto \Delta_\xi \, e^{-\rho_{ij}} \rho_{ij}, \tag{11}$$

where ρ_{ij} is the Agmon distance between basins B_i and B_j. For the sake of simplicity, we retain the notation Δ_ξ for the mean level spacing, as in Eq. (1), even though a unique localization length ξ no longer exists.

The resonance condition of Eq. (8) together with Eq. (7) implies that the states i and j contribute to $\sigma(\omega)$ only if $2t_{ij} \leqslant \hbar\omega$. This imposes a lower bound ρ_ω on the Agmon distance between such states:

$$\rho_{ij} \gtrsim \rho_\omega = \ln \frac{2\Delta_\xi}{\hbar\omega}. \tag{12}$$

Here, ρ_ω is the LL-generalized Mott scale [38]. Beyond ρ_ω, the exponential decay of localized states leads to suppressed contributions to conductance. The Agmon distance is dimensionless, so the range of ρ relevant for conduction at frequency ω is $[\rho_\omega, \rho_\omega + 1]$.

We can now generalize Mott's argument in terms of the Agmon distance. Figure 1 provides a schematic representation of the situation for a fixed value of ω. The small region in the center is the basin B_i of one localized state (of index i). All points located at an Agmon distance $\rho \in [\rho_\omega, \rho_\omega + 1]$ from this basin are plotted in orange. If another localized state lives further or closer than this distance, it cannot hybridize with state i, and thus no hopping occurs between the two states. As a result, conduction essentially operates by resonant-assisted tunneling between pairs of localized states distant by about ρ_ω in Agmon distance. If one imagines the transportation network as a graph whose vertices are the basins of the effective potential, the actual conduction network is obtained by keeping only the edges corresponding to an Agmon distance in $[\rho_\omega, \rho_\omega + 1]$.

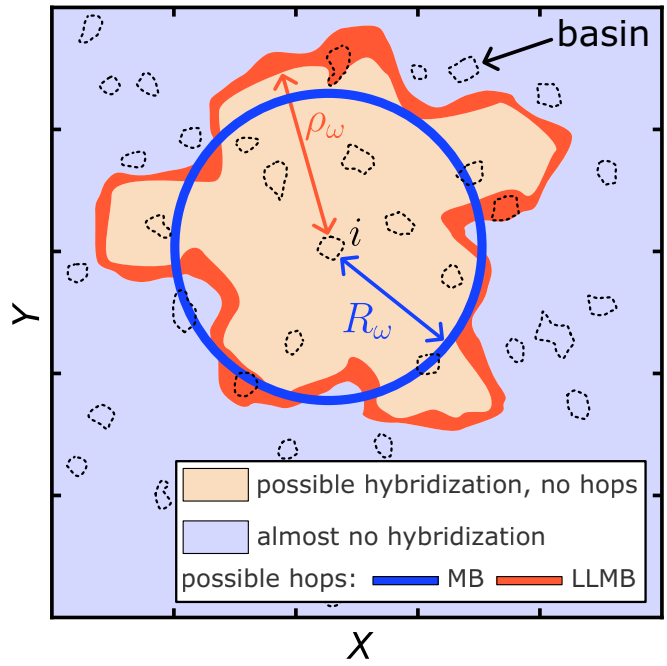

FIG. 1. Schematic of LL approach to ac transport. Basins B_i are displayed by black dashed lines. The orange region is such that $\rho_\omega \leqslant \rho(\vec{r}, B_i) \leqslant \rho_\omega + d\rho$, with $d\rho = 1$. The width of this region is constant in Agmon's distance but not in Euclidean distance. The boundary at the Mott scale R_ω is the blue circle.

IV. ASSESSING THE AC CONDUCTIVITY

Now that we have determined which pairs of states contribute to the conduction through the LL-generalized Mott scale ρ_ω, we are left with estimating the square modulus of the position matrix element $|\boldsymbol{X}_{i,j}|^2$ for these pairs of states. This quantity only depends on the Euclidean distance between basins B_i and B_j, and a rapid computation leads for these states to

$$|\boldsymbol{X}_{i,j}|^2 \approx |\boldsymbol{r}_i - \boldsymbol{r}_j|^2/4. \tag{13}$$

(See Appendix B for details.) For states that do not contribute to the conductivity, $|\boldsymbol{X}_{i,j}|^2 \approx 0$.

We define Σ_ω as the set of state indices i satisfying $|E_i - E_F| \leqslant \hbar\omega$. Other states cannot participate in the conduction. Let us compute the average distribution of Euclidean distance between pairs of states $(i, j) \in \Sigma_\omega^2$ separated by the Agmon distance $\rho_{ij} \in [\rho, \rho + \mathrm{d}\rho]$ and the Euclidean distance $r_{ij} = |\boldsymbol{r}_i - \boldsymbol{r}_j| \in [r, r + \mathrm{d}r]$. This distribution is defined as follows:

$$f(r, \rho) \frac{\mathrm{d}r \, \mathrm{d}\rho}{|\Omega|} = \langle \mathbb{1}_{[r, r+\mathrm{d}r]}(r_{ij}) \times \mathbb{1}_{[\rho, \rho+\mathrm{d}\rho]}(\rho_{ij}) \rangle_{i,j \in \Sigma_\omega}, \tag{14}$$

where $\mathbb{1}_A$ is the characteristic function of a set A, and $f(r, \rho)\,\mathrm{d}r\,\mathrm{d}\rho$ is the average volume filled by the final states contributing to conductivity.

The next step is to determine $|\boldsymbol{X}|^2_{\mathrm{avg}}$, which is obtained by averaging $r^2/4$ with the above distribution:

$$|\boldsymbol{X}|^2_{\mathrm{avg}} = \frac{1}{4|\Omega|} \int_{r=0}^{+\infty} r^2 f(r, \rho) \, \mathrm{d}\rho \, \mathrm{d}r. \tag{15}$$

Recalling that the relevant range $\rho \in [\rho_\omega, \rho_\omega + 1]$, we can rewrite

$$|\boldsymbol{X}|^2_{\text{avg}} = \frac{1}{4|\Omega|}\int_0^\infty r^2 f(r,\rho_\omega)\mathrm{d}r = \frac{1}{4|\Omega|}\mathbb{E}_\omega(X^2). \tag{16}$$

$\mathbb{E}_\omega(X^2)$ is the second moment in r of the distribution f at the LL-generalized Mott scale ρ_ω. In the view of Eq. (3') in Ref. [20], p. 854, $f/|\Omega|$ is an approximation of the two-point correlator given in Eq. (4) in the same paper. In the LL framework, however, only the dominant contributions to this correlator, corresponding to $\rho_{ij} \in [\rho_\omega, \rho_\omega + 1]$, are kept. In addition, f is easier to compute than the correlator as it does not require *a priori* knowledge of the wave functions.

Substituting Eq. (16) into the KG formula of Eq. (4) finally leads to the LL-generalized MB formula:

$$\sigma(\omega) \underset{\omega\longrightarrow 0}{\approx} \frac{\pi e^2\hbar}{2d}\,\nu^2\,\omega^2\,\mathbb{E}_\omega(X^2). \tag{17}$$

The LL enters this formula through the LL-generalized Mott scale ρ_ω that selects participating states.

Computing the conductivity of a system therefore requires to determine $f(r,\rho_\omega)$ and then $\mathbb{E}_\omega(X^2)$, according to the following workflow:

$$\begin{aligned} V \longrightarrow u \longrightarrow V_u \longrightarrow \{B_i\} \longrightarrow \Sigma_\omega \\ \longrightarrow f(r,\rho_\omega) \longrightarrow \mathbb{E}_\omega(X^2) \longrightarrow \sigma(\omega). \end{aligned}$$

This approach generalizes the MB derivation, allowing to investigate systems out of the scope of the MB formula.

As a consistency check, let us recover the MB formula under Mott's assumptions. In Mott's derivation, the Euclidean distance between pairs of states that participate to conduction typically belongs to $[R_\omega, R_\omega + \xi]$, where R_ω is the Mott scale [12,13,39], defined as

$$R_\omega = \xi \ln\frac{2\Delta_\xi}{\hbar\omega}. \tag{18}$$

It can be retrieved from the LL-generalized Mott scale if one assumes that all states at a given energy share the same localization length. In this case, the Agmon distance between two states is simply $\rho_{ij} = r_{ij}/\xi$, and

$$\mathbb{1}_{[\rho_\omega,\rho_\omega+1]}(\rho_{ij}) = \mathbb{1}_{[R_\omega,R_\omega+\xi]}(r_{ij}). \tag{19}$$

This leads to

$$f_{\text{Mott}}(r,\rho_\omega)\,\mathrm{d}r = \begin{cases} S_d\, r^{d-1}\,\mathrm{d}r, & \text{if } R_\omega \leqslant r \leqslant R_\omega + \xi \\ 0, & \text{otherwise} \end{cases}, \tag{20}$$

where S_d is the area of the d-dimensional unit sphere. Indeed, averaging over all pairs of states in Σ^2_ω yields the volume occupied by the final states, which corresponds to the volume of the shell between r and $r + \mathrm{d}r$. Since the basins are considered to be well separated, then $R_\omega \gg \xi$ and

$$\mathbb{E}_\omega(X^2) \approx S_d\, R_\omega^{d+1}\xi = S_d\,\xi^{d+2}\left(\ln\frac{2\Delta_\xi}{\hbar\omega}\right)^{d+1}. \tag{21}$$

We recover here the MB formula from Ref. [22] with an additional factor 2 due to the inclusion of spinful electrons in our model.

V. DISCUSSION AND CONCLUSIONS

Let us emphasize once more differences between the conventional Mott picture and our treatment using the LL. In the MB picture, electronic conduction occurs by hopping between localized states separated by the Euclidean distance R_ω, regardless of the details of the potential in between. The points at a distance equal to the Mott scale from a given localized state form a $(d-1)$ sphere, as depicted in blue in Fig. 1. Yet, two localized states at distance R_ω from each other but separated by a very large potential barrier would not be able to hybridize and contribute to conductivity. Conversely, a pair of states closer to each other than R_ω can participate in transport if a large potential barrier separates them.

These configurations, not accounted for precisely in the MB derivation, are handled in a very general way by the LL through the Agmon distance, which deforms the space geometry to account for the shape of the potential. As a result the region of "active states" is not a Euclidean sphere but its deformed version, shown in orange in Fig. 1. In addition to being more general, the LL-generalized Mott scale also allows us to consider specific realizations of disorder instead of disorder averages.

In conclusion, the LL approach extends the MB formula to systems with statistically isotropic and homogeneous disordered effective potentials, accommodating spatially varying localization lengths. It introduces an extended Mott scale which captures fluctuations of the effective potential. Hops between states occur at Agmon distances defined by this LL-generalized Mott scale, ensuring both hybridization and resonance. In this framework, conductivity is governed by the second moment of the distribution of Euclidean distances between wells separated by approximately ρ_ω in the LL-based Agmon metric.

In this work, we relaxed two fundamental assumptions of the original MB formula: the uniformity of the localization length and the requirement for well-defined wells. Future developments could involve abandoning the assumption of a constant density of states, leveraging LL-based approximations [29]. It could be interesting to look for specific forms of disorder that, through anomalous density of states behavior or nonconventional Agmon distance, would alter the frequency dependence in the Mott-Berezinskiĭ equation, opening the possibility of tailoring conductivity at the nanoscale in such media.

ACKNOWLEDGMENT

M.F. and G.H. are supported by the project Localization of Waves of the Simons Foundation (Grant No. 1027116, M.F.).

DATA AVAILABILITY

No data were created or analyzed in this study.

APPENDIX A: COMPUTING THE TRANSITION AMPLITUDE

We assess the transition amplitude between two ground states $\psi_i^{(1)}$ and $\psi_j^{(1)}$ of the one-well Hamiltonians $H_i^{(1)}$ and

$H_j^{(1)}$, localized in the basins B_i and B_j with energies E_i and E_j, both energies being approximately equal to E_F [22]:

$$t_{ij} = E_F \int_\Omega \psi_j^{(1)*}(\boldsymbol{r})\, \psi_i^{(1)}(\boldsymbol{r})\, \mathrm{d}\boldsymbol{r}. \tag{A1}$$

Replacing both wave functions outside their basins by their approximations obtained from the LL [see Eq. (10)] leads to an expression which can be split into three contributions: one per basin and one in the domain complementary to both basins. This reads

$$\begin{aligned} t_{ij} \approx E_F \Bigg(& c_j \int_{B_i} \psi_i(\boldsymbol{r})\, e^{-\rho(B_j,\boldsymbol{r})} \mathrm{d}\boldsymbol{r} \\ & + c_i \int_{B_j} \psi_j(\boldsymbol{r})\, e^{-\rho(B_i,\boldsymbol{r})} \mathrm{d}\boldsymbol{r} \\ & + c_i\, c_j \int_{\Omega\setminus(B_i\cup B_j)} e^{-\rho(B_i,\boldsymbol{r})-\rho(B_j,\boldsymbol{r})} \mathrm{d}\boldsymbol{r} \Bigg). \end{aligned} \tag{A2}$$

Let us evaluate the last contribution I_{ij}, defined as

$$I_{ij} = \int_{\Omega\setminus(B_i\cup B_j)} e^{-\rho(B_i,\boldsymbol{r})-\rho(B_j,\boldsymbol{r})}\, \mathrm{d}\boldsymbol{r}. \tag{A3}$$

To do so, we use the Laplace method, first introduced by Laplace in 1774 for one-dimensional integrals [40], then extended to multivariate ones [41,42]. This method is the real counterpart of the stationary phase method [43,44] used to approximate complex integrals of the form

$$I(t) = \int_A e^{-f(\boldsymbol{r},t)}\, g(\boldsymbol{r},t)\, \mathrm{d}\boldsymbol{r}, \tag{A4}$$

where A is a subdomain of $\mathbb{R}^d$. In our case $A = \Omega \setminus (B_i \cup B_j)$, $g(\boldsymbol{r},t) = 1$, and $f(\boldsymbol{r},t) = \rho(B_i,\boldsymbol{r}) + \rho(B_j,\boldsymbol{r})$. Both functions f and g are time independent.

By triangular inequality of the Agmon distance, the value of f is always larger than the Agmon distance ρ_{ij} between B_i and B_j. By definition, f is equal to ρ_{ij} on the geodesic of the Agmon distance connecting B_i to B_j:

$$\forall \boldsymbol{r} \in \Gamma_{ij},\ f(\boldsymbol{r}) = \rho(B_i,\boldsymbol{r}) + \rho(B_j,\boldsymbol{r}) = \rho_{ij}. \tag{A5}$$

We assume here that Γ_{ij} is unique everywhere the Agmon metric is nondegenerate, i.e., where $1/u(\boldsymbol{r})$ is larger than E_F. We will see later that our demonstration can be extended to the case of multiple geodesics. The parts of Γ_{ij} where the Agmon distance is degenerate ($1/u < E_F$) correspond to a union of regions $\{\tilde{B}_k\}$. It is easy to assess the contribution of each of these regions to the coupling:

$$\int_{\tilde{B}_k} e^{-f(\boldsymbol{r})} \mathrm{d}\boldsymbol{r} = e^{-\rho_{ij}} \int_{\tilde{B}_k} \mathrm{d}\boldsymbol{r} = e^{-\rho_{ij}} |\tilde{B}_k|, \tag{A6}$$

where $|\tilde{B}_k|$ denotes the volume of the region $\tilde{B}_k$.

One now focuses on the complementary region, the part of the geodesic where the Agmon distance is nondegenerate, hereafter called Γ_1. Starting from any point $\boldsymbol{s}$ of Γ_1, moving orthogonally to Γ_1, i.e., in the hyperplane $\mathcal{P}(\boldsymbol{s})$ orthogonal to the local tangent to Γ_1 at $\boldsymbol{s}$, increases the value of f. We can therefore expand f around a point $\boldsymbol{s}$ of Γ_1, $\boldsymbol{z}$ belonging to $\mathcal{P}(\boldsymbol{s})$:

$$f(\boldsymbol{s}+\boldsymbol{z}) = \rho_{ij} + \tfrac{1}{2}\boldsymbol{z}^T H_\perp(\boldsymbol{s})\, \boldsymbol{z} + o(\|\boldsymbol{z}\|^2), \tag{A7}$$

where $H_\perp(\boldsymbol{s})$ denotes the Hessian of f restricted to $\mathcal{P}(\boldsymbol{s})$. By definition of the geodesic,

$$\forall \boldsymbol{s} \in \Gamma_1, \quad H_\perp(\boldsymbol{s}) > 0. \tag{A8}$$

Using Ref. [45], 3.1.1, (also used in Ref. [46]), allows us then to approximate I_{ij} at the first nonvanishing order:

$$I_{ij} \approx e^{-\rho_{ij}} \left[\int_{\Gamma_1} \frac{(2\pi)^{\frac{d-1}{2}}}{\sqrt{\det(H_\perp(\boldsymbol{s}))}}\, \mathrm{d}\boldsymbol{s} + \sum_k |\tilde{B}_k| \right]. \tag{A9}$$

The narrower the function f around its minimal path, the better the approximation. The quantity $1/\sqrt{\det(H_\perp(\boldsymbol{s}))}$ that appears in the denominator comes from neglecting the high-order contribution in Eq. (A7). We are left in this case with integrating a Gaussian function over the entire local hyperplane. Interestingly, $1/\sqrt{\det(H_\perp(\boldsymbol{s}))} = 1/\sqrt{\prod_\ell \lambda_\ell}$, where $\{\lambda_\ell\}$ are the eigenvalues of the Hessian, i.e., the curvature of the Agmon distance along the various transverse directions. The integrand in the first term of Eq. (A9) can therefore be interpreted as a local effective cross section. A large curvature corresponds to a small cross section, while a small curvature leads to a large cross section.

Once integrated along Γ_1, this cross section gives the effective volume of a d-dimensional tube connecting the various basins $\tilde{B}_k$. Consequently, one can regroup all terms inside the same expression,

$$I_{ij} = e^{-\rho_{ij}}\, V_{ij}, \tag{A10}$$

where V_{ij} denotes the total effective volume of a tube surrounding the geodesic that significantly contributes to the coupling between localized states in basins B_i and B_j. If several geodesics connect both basins, the same method can be extended, summing over all volumes of each geodesic.

Returning to Eq. (A2), we estimate the remaining two terms. The Agmon distances involved are

$$\rho(B_i, \boldsymbol{r} \in B_j) = \rho(B_j, \boldsymbol{r} \in B_i) = \rho(B_i, B_j) = \rho_{ij}. \tag{A11}$$

Using the estimate $\psi_i \sim c_i$ inside B_i, we get that

$$c_j \int_{B_i} \psi_i(\boldsymbol{r})\, e^{-\rho(B_j,\boldsymbol{r})} \mathrm{d}\boldsymbol{r} \sim c_i c_j e^{-\rho_{ij}} |B_i|. \tag{A12}$$

The transition amplitude can now be written as

$$t_{ij} \approx e^{-\rho_{ij}}\, E_F\, c_i c_j (V_{ij} + |B_i| + |B_j|). \tag{A13}$$

Recall that the normalization constant $c_i \sim V_i^{-1/2}$, with V_i the volume occupied by the state $\psi_i^{(1)}$. The effective potential being statistically homogeneous, the volumes occupied by localized states at an energy close to the Fermi energy are comparable. Therefore $c_i\, c_j \approx 1/V_F$, with V_F the volume occupied by a localized state at energy E_F. This volume can be expressed in terms of the mean level spacing Δ_ξ,

$$\Delta_\xi = \frac{1}{V_F\, \nu}, \quad \text{hence} \quad c_i\, c_j \approx \Delta_\xi\, \nu. \tag{A14}$$

The transition amplitude now reads

$$t_{ij} \approx \Delta_\xi e^{-\rho_{ij}}\, \nu E_F (V_{ij} + |B_i| + |B_j|). \tag{A15}$$

The product $\nu E_F = n$ is, roughly, the density of carriers, and then $N_i = n|B_i|$ represents the number of carriers inside the basin B_i, which is independent of the frequency ω.

On the other hand, the number of carriers inside the tube surrounding the Agmon geodesic $N_{ij} = nV_{ij} \propto \rho_{ij}$. For the states of interest in this paper, the Agmon distance $\rho_{ij} \gg 1$. Thus, $N_{ij} \gg N_i, N_j$, and the final estimate of the transition amplitude is

$$t_{ij} \propto \Delta_\xi \rho_{ij} e^{-\rho_{ij}}, \tag{A16}$$

with dimensionless prefactor independent of ω.

In 2D and approximately in 3D, one can go one step further and assess the value of the local cross section along the geodesic. To that end, one needs to estimate $\det(H_\perp(\boldsymbol{s}))$, see Eq. (A9). This is done by plugging the estimate from Eq. (10) into the Schrödinger equation:

$$\frac{\hbar^2}{2m}\Delta\rho - \frac{\hbar^2}{2m}|\nabla\rho|^2 + V \approx E. \tag{A17}$$

The eikonal equation satisfied by the Agmon distance $|\nabla\rho|^2 = \frac{2m}{\hbar^2}(\frac{1}{u} - E)_+$ yields the value of $\Delta\rho$ wherever $1/u \geqslant E$:

$$\frac{\hbar^2}{2m}\Delta\rho \approx \frac{1}{u} - V, \quad \text{hence} \quad \Delta\rho \approx -\frac{\Delta u}{u}. \tag{A18}$$

The eigenvalue of the aforementioned Hessian $H_\perp$ vanishes along the direction of the geodesic. In 2D, this gives $\Delta\rho(\boldsymbol{s}) = \lambda_\parallel + \lambda_\perp = \lambda_\perp = \det(H_\perp(\boldsymbol{s}))$; hence,

$$\det(H_\perp(\boldsymbol{s})) \approx -\frac{\Delta u(\boldsymbol{s})}{u(\boldsymbol{s})}. \tag{A19}$$

In 3D, $\Delta\rho(\boldsymbol{s}) = \lambda_{\perp,1} + \lambda_{\perp,2}$. Moreover, $\lambda_{\perp,1} \approx \lambda_{\perp,2} \approx \lambda_\perp$ due to the stastitical isotropy. This yields

$$\det(H_\perp(\boldsymbol{s})) \approx \lambda_\perp^2 \approx \frac{1}{4}\left(\frac{\Delta u(\boldsymbol{s})}{u(\boldsymbol{s})}\right)^2. \tag{A20}$$

APPENDIX B: DERIVATION OF THE MATRIX ELEMENT

One can express the wave functions, $\psi_\pm$ of the two-well Hamiltonian in terms of $\psi_i^{(1)}$ and $\psi_j^{(1)}$ [22]:

$$\psi_+ = \cos(\theta)\,\psi_i^{(1)} + \sin(\theta)\,\psi_j^{(1)}, \tag{B1}$$

$$\psi_- = -\sin(\theta)\,\psi_i^{(1)} + \cos(\theta)\,\psi_j^{(1)}, \tag{B2}$$

where θ is a mixing angle such that $\tan(\theta) = \frac{t_{ij}}{\delta + \sqrt{t_{ij}^2 + \delta^2}}$ with $\delta = \frac{E_i - E_j}{2}$. For instance, the matrix element along direction Ox reads

$$X_{i,j}^{(x)} = \int \psi_+^*(\boldsymbol{r})\, x\, \psi_-(\boldsymbol{r})\mathrm{d}\boldsymbol{r} = \frac{t_{ij}}{2\sqrt{t_{ij}^2 + \delta^2}}(x_j - x_i) + \frac{\delta}{\sqrt{t_{ij}^2 + \delta^2}} \int \psi_i^{(1)}(\boldsymbol{r})\, x\, \psi_j^{(1)}(\boldsymbol{r})\mathrm{d}\boldsymbol{r}. \tag{B3}$$

For states that hybridize, $t_{ij} \gg \delta$ and the second term is negligible. For states that do not hybridize, the overlap is very small and the contribution of theses states to the average is negligible. In a statistically isotropic and homogeneous medium, the square matrix element reads

$$|\boldsymbol{X}_{i,j}|^2 = \sum_{\alpha=1}^{d} \left|X_{i,j}^{(\alpha)}\right|^2, \tag{B4}$$

where the sum runs over all directions of space. Consequently, $|\boldsymbol{X}_{i,j}|^2 \approx \frac{|\boldsymbol{r}_i - \boldsymbol{r}_j|^2}{4}$ between states that contribute to conduction, whereas $|\boldsymbol{X}_{i,j}|^2 \approx 0$ between states that do not.

[1] M. Pollak, in *Proceedings of the 5th International Conference on Amorphous and Liquid Semiconductors*, Garmisch-Partenkirchen 1973 (Taylor and Francis, London, 1974).

[2] I. I. Fishchuk and V. N. Rudko, Low-frequency conductivity in disordered systems due to variable-range hopping, J. Phys. C: Solid State Phys. **13**, L493 (1980).

[3] S. Elliott, A.c. conduction in amorphous chalcogenide and pnictide semiconductors, Adv. Phys. **36**, 135 (1987).

[4] A. G. Hunt, Ac hopping conduction: Perspective from percolation theory, Philos. Mag. B **81**, 875 (2001).

[5] B. I. Shklovskii and A. L. Efros, *Electronic Properties of Doped Semiconductors*, Vol. 45 (Springer, Berlin, 1984).

[6] S. V. Syzranov, L. Radzihovsky, and V. Gurarie, Critical transport in weakly disordered semiconductors and semimetals, Phys. Rev. Lett. **114**, 166601 (2015).

[7] S. Tanaka and H. Y. Fan, Impurity conduction in *p*-type silicon at microwave frequencies, Phys. Rev. **132**, 1516 (1963).

[8] J. Blinowski and J. Mycielski, Theory of absorption of electromagnetic radiation by hopping in *n*-type silicon and germanium, Phys. Rev. **136**, A266 (1964).

[9] J. Blinowski and J. Mycielski, Theory of absorption of electromagnetic radiation by hopping in *n*-type silicon and germanium. II, Phys. Rev. **140**, A1024 (1965).

[10] N. F. Mott, Conduction in non-crystalline systems, Philos. Mag. **17**, 1259 (1968).

[11] N. F. Mott, Conduction in non-crystalline systems, Philos. Mag. **22**, 7 (1970).

[12] N. F. Mott, Conduction in non-crystalline systems I. Localized electronic states in disordered systems, in *Sir Nevill Mott–65 Years in Physics*, World Scientific Series in 20th Century Physics (World Scientific, Singapore, 1995), pp. 429–439.

[13] N. F. Mott and E. A. Davis, *Electronic Processes in Non-Crystalline Materials* (Oxford University Press, 2012).

[14] V. L. Berezinskiĭ, Kinetics of a quantum particle in a one-dimensional random potential, Zh. Eksp. Teor. Fiz. **11**, 87 (1996).

[15] P. W. Anderson, Absence of diffusion in certain random lattices, Phys. Rev. **109**, 1492 (1958).

[16] A. A. Abrikosov and I. A. Ryzhkin, Conductivity of quasi-one-dimensional metal systems, Adv. Phys. **27**, 147 (1978).

[17] I. M. Lifshitz, S. A. Gredeskul, and L. A. Pastur, *Introduction to the Theory of Disordered Systems* (Wiley, 1988).

[18] A. Houghton, L. Schäfer, and F. J. Wegner, Two-particle spectral function and ac conductivity of an amorphous system far below the mobility edge: A problem of interacting instantons, Phys. Rev. B **22**, 3598 (1980).

[19] R. Hayn and W. John, Instanton approach to the conductivity of a disordered solid, Nucl. Phys. B **348**, 766 (1991).

[20] L. P. Gor'kov, O. N. Dorokhov, and F. V. Prigara, Structure of wave functions and ac conductivity in disordered one-dimensional conductors, Zh. Eksp. Teor. Fiz. **85**, 1470 (1983).

[21] D. A. Ivanov, M. A. Skvortsov, P. M. Ostrovsky, and Y. V. Fominov, Hybridization of wave functions in one-dimensional localization, Phys. Rev. B **85**, 035109 (2012).

[22] W. Kirsch, O. Lenoble, and L. Pastur, On the Mott formula for the ac conductivity and binary correlators in the strong localization regime of disordered systems, J. Phys. A: Math. Gen. **36**, 12157 (2003).

[23] A. Klein, O. Lenoble, and P. Müller, On Mott's formula for the ac-conductivity in the Anderson model, Ann. Math. **166**, 549 (2007).

[24] G. M. Falco, A. A. Fedorenko, and I. A. Gruzberg, Wave function correlations and the AC conductivity of disordered wires beyond the Mott-Berezinskii law, Europhys. Lett. **120**, 37004 (2017).

[25] G. M. Falco, A. A. Fedorenko, and I. A. Gruzberg, On functional determinants of matrix differential operators with multiple zero modes, J. Phys. A: Math. Theor. **50**, 485201 (2017).

[26] I. A. Gruzberg and A. Nahum (unpublished).

[27] M. Filoche and S. Mayboroda, Universal mechanism for Anderson and weak localization, Proc. Natl. Acad. Sci. USA **109**, 14761 (2012).

[28] G. David, M. Filoche, and S. Mayboroda, The landscape law for the integrated density of states, Adv. Math. **390**, 107946 (2021).

[29] D. N. Arnold, G. David, D. Jerison, S. Mayboroda, and M. Filoche, Effective confining potential of quantum states in disordered media, Phys. Rev. Lett. **116**, 056602 (2016).

[30] D. N. Arnold, G. David, M. Filoche, D. Jerison, and S. Mayboroda, Computing spectra without solving eigenvalue problems, SIAM J. Sci. Comput. **41**, B69 (2019).

[31] M. Filoche, M. Piccardo, Y.-R. Wu, C.-K. Li, C. Weisbuch, and S. Mayboroda, Localization landscape theory of disorder in semiconductors. I. Theory and modeling, Phys. Rev. B **95**, 144204 (2017).

[32] M. Piccardo, C.-K. Li, Y.-R. Wu, J. S. Speck, B. Bonef, R. M. Farrell, M. Filoche, L. Martinelli, J. Peretti, and C. Weisbuch, Localization landscape theory of disorder in semiconductors. II. Urbach tails of disordered quantum well layers, Phys. Rev. B **95**, 144205 (2017).

[33] C.-K. Li, M. Piccardo, L.-S. Lu, S. Mayboroda, L. Martinelli, J. Peretti, J. S. Speck, C. Weisbuch, M. Filoche, and Y.-R. Wu, Localization landscape theory of disorder in semiconductors. III. Application to carrier transport and recombination in light emitting diodes, Phys. Rev. B **95**, 144206 (2017).

[34] A. Thayil and M. Filoche, Realization-dependent model of hopping transport in disordered media, Appl. Phys. Lett. **123**, 252102 (2023).

[35] M. Filoche, P. Pelletier, D. Delande, and S. Mayboroda, Anderson mobility edge as a percolation transition, Phys. Rev. B **109**, L220202 (2024).

[36] S. Agmon, *Lectures on Exponential Decay of Solutions of Second-Order Elliptic Equations: Bounds on Eigenfunctions of N-Body Schrödinger Operations*, Mathematical Notes, Vol. 29 (Princeton University Press, Princeton, NJ, 1982).

[37] S. Agmon, Bounds on exponential decay of eigenfunctions of Schrödinger operators, in *Schrödinger Operators*, edited by S. Graffi (Springer, 1985), pp. 1–38.

[38] A more accurate estimate results from inverting Eq. (11) using the Lambert W function: $\rho_{ij} \approx -W_1(-t_{ij}/\Delta_\xi) \gtrsim -W_1(-\hbar\omega/2\Delta_\xi)$. For $x \ll 1$ one can use the asymptotic expansion $W_1(-x) = \ln(-x) - \ln(-\ln(-x)) + \mathrm{o}(1)$.

[39] N. F. Mott, Electrons in disordered structures, Adv. Phys. **16**, 49 (1967).

[40] P. S. de Laplace, Mémoire sur la Probabilité des Causes par les Evénements, in *Mémoires de l'Académie Royale des Sciences de Paris*, Tome VI (Académie Royale des Sciences de Paris, 1774), p. 621.

[41] R. Wong, Double integrals, in *Asymptotic Approximations of Integrals* (Society for Industrial and Applied Mathematics, 2001), Chap. 8, pp. 423–476.

[42] T. M. Łapiński, Multivariate Laplace's approximation with estimated error and application to limit theorems, J. Approx. Theory **248**, 105305 (2019).

[43] V. I. Arnold, Remarks on the stationary phase method and Coxeter numbers (Volume 28, 1973), in *Singularity Theory*, London Mathematical Society Lecture Note Series (Cambridge University Press, 1981), pp. 61–90.

[44] J. J. Duistermaat, Global theory of Fourier integral operators, in *Fourier Integral Operators* (Birkhäuser Boston, Boston, 2011), pp. 91–112.

[45] M. Ludewig, Path integrals on manifolds with boundary, Commun. Math. Phys. **354**, 621 (2017).

[46] M. Ludewig, Heat kernel asymptotics, path integrals and infinite-dimensional determinants, J. Geom. Phys. **131**, 66 (2018).